ELSEVIER

Journal of Petroleum Science and Engineering 12 (1995) 171–181

PETROLEUM SCIENCE & ENGINEERING

Analysis of pressure and pressure derivative without type-curve matching — Skin and wellbore storage

Djebbar Tiab

School of Petroleum and Geological Engineering, The University of Oklahoma, 100 East Boyd Street, T301 SEC, Norman, OK 73019-0628, USA

Received 6 March 1994; accepted 15 July 1994

Abstract

The current type-curve matching technique is essentially a trial-and-error procedure. A new technique for interpreting pressure tests using log–log plots of the pressure and pressure derivative versus time to calculate reservoir and well parameters *without* type-curve matching is presented. This paper concentrates on the interpretation of pressure tests in which wellbore storage and skin are present. Characteristic points are obtained of intersection of various straight line portions of the pressure and pressure derivative curve, slopes and starting times of these straight lines. These points, slopes and times are then used with appropriate equations to solve directly for permeability, wellbore storage and skin. A step-by-step procedure for calculating these parameters without type-curve matching for five different cases is included in the paper.

The most important aspect of this new technique is its accuracy because it uses exact analytical solutions to calculate permeability, skin, and wellbore storage. The proposed technique is applicable to the interpretation of pressure buildup and drawdown tests and is illustrated by several numerical examples.

1. Introduction and basic equations

Interpretation of pressure tests for a single well with wellbore storage and skin in a homogeneous reservoir considerably improved when the type-curve matching technique was published in the seventies (Ramey, 1970; Agarwal et al., 1970; Ramey and Agarwal, 1972; Earlougher and Kersch, 1974). Later that decade Tiab introduced the pressure derivative analysis (Tiab, 1975, 1976; Tiab and Crichlow, 1979; Tiab and Kumar, 1980a, b; Puthigai and Tiab, 1982). He showed that a log–log plot of pressure derivative versus time is an important tool in identifying flow regimes and boundary effects. In the eighties type-curves which combine both the pressure and pressure derivative functions for various reservoir systems became an integral part of modern well test analysis (Bourdet et al., 1983; Clark and Van Golf-Racht, 1984; Wong et al., 1986; Ozkan et al., 1987; Mishra and Ramey, 1988; Onur and Reynolds, 1988; Vongvuthipornchai and Raghavan, 1988; Horne, 1990). Unless all flow regimes are definitely observed in the pressure derivative curve, type-curve matching is still a risky technique. Also, combinations of various boundary conditions may yield approximately similar pressure behavior. For a well producing from a bounded system, it is possible for inner and outer boundary effects to interact and considerably affect the well pressure behavior such that the infinite acting radial flow line is either too short or non-existent. Horne (1990) showed that log–log type curve matching is not as accurate as conventional semilog methods, because log–log axes tend to mask inaccuracies at late time, where 1 mm deviation of a pressure point may mean an actual error of 200 psia. Finally, the noise in

This paper was originally presented as SPE 25426 at the 1993 SPE Production Operations Symp., March 21–23, Oklahoma City, Okla.
SSDI 0920-4105(94)00040-9

the pressure derivative curve can be sever enough to make it impossible to draw the characteristic straight lines corresponding to flow regimes.

In this paper, it is shown how a log–log plot of pressure and pressure derivatives versus time can be analyzed without using the type-curve matching technique. This new approach is particularly useful when the early-time unit slope line and/or the late-time infinite acting radial flow line are not well developed due to the lack of points or any of the reasons discussed above. This new technique is also applicable to hydraulically fractured wells (Tiab, 1989, 1993). The classical assumptions normally used in conjunction with a single well producing at a constant rate from a homogeneous, isotropic and uniform porous media are applicable in this study. The fluid has a constant viscosity and is considered to be slightly compressible. The dimensionless wellbore pressure for a well with storage and skin, p_{wD}, and its derivative, dp_{wD}/dt, are obtained from

$$p_D = \frac{4}{\pi^2}\int_0^\infty \left(\frac{1 - e^{-u^2 t_D}}{u^3 U_J}\right) du \tag{1.1}$$

and

$$\frac{dp_{wD}}{dt_D} = \frac{4}{\pi^2}\int_0^\infty \left(\frac{e^{-u^2 t_D}}{u U_J}\right) du \tag{1.2}$$

where

$$U_J = [uC_D J_0(u) - (1 - C_D s u^2) J_1(u)]^2 + (uC_D Y_0(u) - (1 - C_D s u^2) Y_1(u)]^2 \tag{1.3}$$

The dimensionless pressure, p_{wD}, dimensionless time, t_D, and dimensionless wellbore storage coefficient are expressed as follows:

$$P_D = \left(\frac{kh}{141.2 q \mu B}\right)\Delta p \tag{1.4}$$

$$t_D = \left(\frac{0.0002637 k}{\phi \mu c_t r_w^2}\right) t \tag{1.5}$$

$$C_D = \left(\frac{0.8935}{\phi c_t h r_w^2}\right) C \tag{1.6}$$

The factors C and s are respectively the wellbore storage coefficient and skin.

2. Characteristic points and straight lines

The log–log plot of dimensionless pressure and pressure derivatives versus time, Fig. 1, has several unique features:

(1) The pressure curve has a unit slope line during early time. This line corresponds to pure wellbore storage flow. The equation of this straight line is

$$p_D = \frac{t_D}{C_D} \tag{2.1}$$

Combining Eqs. 1.5 and 1.6 gives

$$\frac{t_D}{C_D} = \left(2.95 \times 10^{-4}\frac{h}{\mu}\right)\frac{t}{C} \tag{2.2}$$

Substituting Eqs. 1.4 and 2.2 into Eq. 2.1 and solving for the wellbore storage coefficient C we obtain

$$C = \left(\frac{qB}{24}\right)\frac{t}{\Delta p} \tag{2.3}$$

For drawdown tests, $\Delta p = p_i - p_{wf}$ and for buildup tests $\Delta p = p_{ws} - p_{wf}$ ($\Delta t = 0$).

(2) The pressure derivative curve also has an early time straight line of unit slope. The equation of this line is obtained by taking the derivative of Eq. 2.1 with respect to the natural log of t_D/C_D. Thus:

$$\left(\frac{t_D}{C_D}\right) p_D' = \frac{t_D}{C_D} \tag{2.4}$$

where the dimensionless pressure derivative is

$$p_D' = \left(\frac{26.856 r_w^2 \phi c_t h}{qB}\right)\Delta p' \tag{2.5}$$

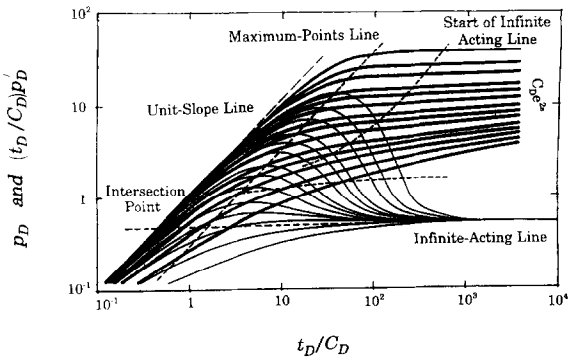

Fig. 1. Characteristics of pressure and pressure derivative type curves.

The left-hand side of Eq. 2.4 can be expressed in real units by combining Eqs. 2.2 and 2.5

$$\left(\frac{t_D}{C_D}\right)p_D' = \left(\frac{kh}{141.2q\mu B}\right)t*\Delta p' \tag{2.6}$$

It is obvious from Fig. 1 that the early-time unit slope line is the same for both pressure and pressure derivative curves. Combining Eqs. 2.4, 2.5 and 2.6 and solving for C we obtain an equation similar to Eq. 2.3 where Δp is replaced with $t*\Delta p'$.

(3) The infinite acting radial flow portion of the pressure derivative is a horizontal straight line. For a homogeneous reservoir, the equation of this line is:

$$\left[\left(\frac{t_D}{C_D}\right)p_D'\right]_r = 0.5 \tag{2.7}$$

Combining Eqs. 2.6 and 2.7 and solving for the permeability yields:

$$k = \frac{70.6q\mu B}{h(t*\Delta p')_r} \tag{2.8}$$

where the subscript r stands for radial flow line. In terms of pressure, the equation of this line is:

$$p_{Dr} = 0.5\left[\ln\left(\frac{t_D}{C_D}\right)_r + 0.80907 + \ln\left(C_D e^{2s}\right)\right] \tag{2.9}$$

(4) The starting time of the infinite acting line of the pressure derivative curve is approximately given by

$$\left(\frac{t_D}{C_D}\right)_{SR} = 10\log\left(C_D e^{2s}\right)^{10} \tag{2.10}$$

This equation is obtained by plotting the values of t_D/C_D corresponding to the first point where Eq. 2.9 is valid, i.e. at the start of the horizontal line for different values of $C_D e^{2s} > 10^2$. Values of $(t_D/C_D)_{SR}$ were obtained from the second derivative of Eq. 1.1. Substituting for C_D and t_D and solving for t_{SR} gives:

$$t_{SR} = \frac{\mu C}{6.9\times10^{-5}kh}\left[\ln\left(\frac{0.8935C}{\phi c_t h r_w^2}\right) + 2s\right] \tag{2.11}$$

where t_{SR} is the starting time of the infinite acting radial flow line.

Vongvuthipornchai and Raghavan (1988) showed that the starting time of the semilog straight line is best determined from

$$\left(\frac{t_D}{C_D}\right)_{SR} = \frac{1}{\alpha}\left[\ln\left(C_D e^{2s}\right) + \ln\left(\frac{t_D}{C_D}\right)_{SR}\right] \tag{2.12}$$

where α is the tolerance (fraction) used to determine the value of t_{DSR} at which Eq. 2.7 is valid. For $\alpha = 0.05$ they found that Eq. 2.12 (approximate solution) can predict the value of t_{DSR} within 8 percent of the value predicted by Eq. 1.2 (exact solution).

The semilog straight line will always appear to start earlier than the horizontal portion of the pressure derivative curve. The difference can be as much as fifty percent.

The wellbore storage coefficient may be estimated from Eq. 2.12 by letting $\alpha = 0.05$ and solving for C:

$$C = 0.056\phi c_t h r_w^2\left(\frac{t_{DSR}}{2s + \ln t_{DSR}}\right) \tag{2.13}$$

where t_{DSR} is calculated from Eq. 1.5 at $t = t_{SR}$.

(5) The early-time unit slope line and the late-time infinite acting line of the pressure derivative, i.e. the horizontal line, intersect at:

$$\left(\frac{t_D}{C_D}p_D'\right)_i = 0.5 \tag{2.14}$$

$$\left(\frac{t_D}{C_D}\right)_i = 0.5 \tag{2.15}$$

where the subscript i stands for "intersection". In real units the coordinates of this intersection point are obtained from

$$(t*\Delta p')_i = \frac{70.6q\mu B}{kh} \tag{2.16}$$

and

$$t_i = \frac{1695\mu C}{kh} \tag{2.17}$$

These equations can be derived, respectively, from Eqs. 2.8, 2.2 and 2.15. Thus, the intersection point can be used to determine k from Eq. 2.16 and C from Eq. 2.17. Since the unit slope line is the same for pressure and pressure derivative curves, at the intersection point we have:

$$(\Delta p)_i = (t*\Delta p')_i = (t*\Delta p')_r \tag{2.18}$$

(6) Between the early-time and late-time straight lines, the derivative curves have specific shapes for different values of $C_D e^{2s}$. In this study, the coordinates of the "peaks" for $C_D e^{2s} > 10^2$ were obtained from the

second derivative and plotted on a cartesian graph. The equation of this line is

$$\left(\frac{t_D}{C_D}p_D'\right)_x = 0.36\left(\frac{t_D}{C_D}\right)_x - 0.42 \quad (2.19)$$

Combining Eqs. 2.2, 2.6 and 2.19 yields:

$$(t*\Delta p')_x = \left(0.015\frac{qB}{C}\right)t_x - 0.42b_x \quad (2.20)$$

where b_x is given by

$$b_x = 141.2q\mu B/kh \quad (2.21)$$

and $(t*\Delta p')_x$ and t_x are the coordinates of the maximum point (peak) of the pressure derivative curve. It is obvious from Eq. 2.20 that we can calculate the wellbore storage coefficient or the permeability from the coordinates of the peak.

Solving Eq. 2.20 for k yields:

$$k = \left(\frac{59.3q\mu B}{h}\right)\frac{1}{(0.015qB/C)t_x - (t*\Delta p')_x} \quad (2.22a)$$

This equation should be used to calculate k only if the late-time infinite acting radial flow line is not observed, such as in a short test, or there is too much noise in the late-time derivative values.

Solving Eq. 2.20 for C yields:

$$C = \frac{0.015qBt_x}{(t*\Delta p')_x + 0.42b_x} \quad (2.22b)$$

This equation should be used in cases where k is known from other sources and the early time unit slope line is not observed.

(7) A log–log plot of $\log(C_De^{2s})$ versus the coordinates of the peaks yielded the following equations:

$$\log\,(C_De^{2s}) = 0.35\left(\frac{t_D}{C_D}\right)_x^{1.24} \quad (2.23)$$

and

$$\log\,(C_De^{2s}) = 1.71\left(\frac{t_D}{C_D}p_D'\right)_x^{1.10} \quad (2.24)$$

Substituting Eqs. 2.2 and 2.6 into Eqs. 2.23 and 2.24 yields two new expressions. Combining these new expressions with Eqs. 2.16 and 2.17 gives:

$$\log C_De^{2s} = 0.1485\left(\frac{t_x}{t_i}\right)^{1.24} \quad (2.25)$$

and

$$\log C_De^{2s} = 0.80\left[\frac{(t*\Delta p')_x}{(t*\Delta p')_i}\right]^{1.10} \quad (2.26)$$

Thus the coordinates of the maximum point (peak) of the pressure derivative can be used also to calculate skin. Solving for skin Eqs. 2.25 and 2.26 give respectively:

$$s = 0.171\left(\frac{t_x}{t_i}\right)^{1.24} - 0.5\ln\left(\frac{0.8935C}{\phi hc_tr_w^2}\right) \quad (2.27)$$

and

$$s = 0.921\left[\frac{(t*\Delta p)_x}{(t*\Delta p)_i}\right]^{1.1} - 0.5\ln\left(\frac{0.8935C}{\phi hc_tr_w^2}\right) \quad (2.28)$$

Because in some pressure tests the wellbore storage hump may appear to be flat at the "peak", it is possible to read the right value of $(t*\Delta p')_x$ but the wrong value of t_x. In this case, it is a good practice to calculate s from both equations. If they give different values then obtain a new value of t_x and repeat the calculations until the two equations give the same value of skin.

(8) An expression relating the infinite-acting radial flow line portion of the pressure derivative curve and the peaks for different values of C_De^{2s} can be derived by dividing Eq. 2.19 with Eq. 2.7:

$$\frac{\left(\frac{t_D}{C_D}p_D'\right)_x}{\left(\frac{t_D}{C_D}p_D'\right)_r} = \frac{1}{0.5}\left[0.36\left(\frac{t_D}{C_D}\right)_x - 0.42\right] \quad (2.29)$$

Using Eqs. 2.2 and 2.6 with Eq. 2.29 we have:

$$\frac{(t*\Delta p')_x}{(t*\Delta p')_r} = 2\left[1.062\times10^{-4}\left(\frac{kh}{\mu}\right)\frac{t_x}{C} - 0.42\right] \quad (2.30)$$

Eq. 2.30 can be used to calculate C or k. Substituting for kh/μ from Eq. 2.8 and solving for C gives:

$$C = \frac{0.015qBt_x}{(t*\Delta p')_x + 0.84(t*\Delta p')_r} \quad (2.31)$$

Thus, the wellbore storage coefficient can be determined even if the unit slope line is not observed for mechanical reasons or due to lack of early time pressure data. Solving for k Eq. 2.30 yields:

$$k = 9416.2\frac{\mu C}{ht_x}\left[0.5\frac{(t*\Delta p')_x}{(t*\Delta p')_r} + 0.42\right] \quad (2.32)$$

(9) An expression relating the infinite-acting radial flow line portions of the pressure and pressure derivative curves can be derived by dividing Eq. 2.9 with Eq. 2.7:

$$\frac{p_{Dr}}{(t_D/C_D)p_D')_r} = \ln t_{Dr} + 2s + 0.80907 \qquad (2.33)$$

Using Eqs. 1.4, 2.2 and 2.6 with Eq. 2.33 and solving for skin we have:

$$s = 0.5\left[\frac{\Delta p_r}{(t*\Delta p')_r} - \ln\left(\frac{kt_r}{\phi\mu c_t r_w^2}\right) + 7.43\right] \qquad (2.34)$$

where t_r is any convenient time during the infinite acting radial flow line and Δp_r is the value of Δp corresponding to t_r.

3. Procedures

Normally, a well designed single-well pressure test in a homogeneous reservoir will show all the necessary flow regimes to determine permeability, skin and wellbore storage from conventional semilog analysis techniques. However, in many cases conventional techniques cannot be used for various reasons: the test is too short to observe the infinite-acting radial flow line, or the wellbore storage unit-slope line is not observed because of lack of early-time pressure points, or there is too much noise in the pressure derivative curve, or both the unit-slope line and the infinite-acting line are missing. In such cases type-curve matching was the only alternative to conventional semilog techniques. However, even with the addition of the pressure derivative curve, finding a unique match by a simple comparison of shapes is still one of the main problems of the type-curve matching technique. The technique proposed here analyzes log–log plots of pressure and pressure derivatives versus time without type-curve matching. The five cases discussed below, with examples, illustrate the effectiveness and simplicity of this new technique.

3.1. Case 1 (basic case) — Unit-slope and infinite-acting lines are observed

The following step-by-step procedure is for the ideal case where both the early time unit-slope line and the late time infinite acting radial flow line have **definitely** been observed, and are **well defined.**

Step 1 — Plot Δp and $t*\Delta p'$ versus time on a log–log graph.

Step 2 — Draw the unit-slope line corresponding to the wellbore storage flow regime using early-time pressure and pressure derivative points. If there is too much noise in the derivative values, it is recommended to draw the unit-slope line using only pressure points.

Step 3 — Draw the infinite acting radial flow line using late-time pressure derivative points. This line is, of course, horizontal.

Step 4 — Read the coordinates of the point where the unit-slope line and the infinite-acting horizontal line intersect: t_i and Δp_i . Note that $\Delta p_i = (t*\Delta p')_i = (t*\Delta p')_r$ in all steps.

Step 5 — Read the coordinates of the maximum point (peak) on the pressure derivative curve: t_x and $(t*\Delta p')_x$.

Step 6 — Select any convenient time t_r during infinite acting radial flow and read Δp_r from the pressure curve.

Step 7 — Calculate the permeability from Eq. 2.8.

Step 8 — Calculate the wellbore storage coefficient from Eq. 2.3 using t_i and Δp_i, or any convenient t and Δp values on the unit slope line.

Step 9 — Calculate the skin factor from Eq. 2.34.

Step 10 — This step is used to verify the correctness and accuracy of the permeability, skin and wellbore storage. This step is necessary only if there is considerable noise in the pressure derivative value. Recalculate permeability using Eq. 2.32. If the values of k obtained from Eqs. 2.8 and 2.32 are approximately equal, this means the peak, the unit-slope and horizontal lines are in their correct "location", and therefore, the values of k, s and C are correct. However, if the two values of k are significantly different, obtain a new peak and/or shift one or both straight lines and repeat Steps 4 through 9 until the values of t_i and Δp_i give similar values of k. The decision of which straight lines should be shifted or whether a new peak should be obtained is really a function of the quality of data. For instance, if the infinite-acting line (horizontal line) portion of the derivative curve is well defined, the value of k and s obtained in Steps 7 and 9 are correct. In this case the unit slope line should be shifted and/or a new peak selected and a new value of C calculated such that the

value of k obtained from Eq. 2.32 is similar to the one obtained in Step 7.

Example 1

A pressure drawdown test in a new oil well is strongly influenced by skin and wellbore storage. The measured pressure data as a function of time are listed in page 156 of Horne. Other known reservoir and well data are:

$q = 2500$ STB/D, $\phi = 0.21$,

$\mu = 0.92$ cp, $c_t = 8.72 \times 10^{-6}$ psi^{-1},

$B = 1.21$ RB/STB, $h = 23$ ft,

$r_w = 0.401$ ft, $p_i = 6009$ psi

Calculate permeability, skin factor and wellbore storage coefficient.

Solution

Figs. 2a and 2b are log–log plots of Δp and $t * \Delta p'$ versus time. The late-time pressure derivative portion in Fig. 2a was calculated by the spline technique (Lane et al., 1991), while the derivative curve in Fig. 2b was calculated by the more commonly used numerical differentiation method (Bourdet et al., 1989). Fig. 2a is used to illustrate Steps 1 through 9 of this case while Fig. 2b is used to illustrate the importance of Step 10. Applying the recommendations in Steps 1 through 6 to Fig. 2a, we obtain:

$t_i = 1.35 \times 10^{-2}$ h, $(t * \Delta p')_r = 110$ psi

$t_x = 0.36$ h, $(t * \Delta p')_x = 965$ psi

$t_r = 10.4$ h, $(\Delta p)_r = 2947$ psi

Using Eq. 2.8 (Step 7), the permeability is 77.6 md. The wellbore storage coefficient is computed from Eq. 2.3 (Step 8) at t_i and Δp_i. Thus, $C = 0.0154$ bbl/psi. Eq. 2.34 (Step 9) gives a skin factor of 6.2. Since the noise in the derivative curve of Fig. 2a is negligible, Step 10 may not be necessary. However, it is a good practice to recalculate k anyway. Using Eq. 2.30, $k = 77.4$ md. Since Eqs. 2.8 and 2.30 give practically the same value of permeability, we can conclude that the values of k, s and C are correct.

Similar results were obtained from Fig. 2b. However, because of the noise in the late-time pressure derivative curve, it took several iterations to find the correct "location" of the horizontal line. In this example, it was not necessary to shift the unit-slope line or the maximum point, as they are well defined. The computer program, however, can shift any of the three characteristic features, i.e. the unit-slope line, the maximum point and the infinite acting line, then recalculate k, C and s until the requirement in Step 10 is satisfied. That is, until Eqs. 2.8 and 2.30 give similar values of permeability. The values of k, C and s obtained here are similar to the values obtained by type-curve matching and semi-log analysis (Horne, 1990).

3.2. Case 2 — The unit-slope line is not observed

Pure wellbore storage flow regime, which causes the early-time pressure and pressure derivative points to yield a unit slope line is not a very common occurrence. Also, in many pressure tests there are not enough early-time points to draw the unit slope line. In this case, the following step-by-step procedure is recommended.

Step 1 — Plot Δp and $t * \Delta p'$ versus time on a log–log graph.

Step 2 — Draw the infinite acting radial flow line (horizontal line) using the late-time pressure derivative points, and read its corresponding value on the pressure derivative axis $(t * \Delta p')_r$. This value is of course equal to $(t * \Delta p')_i$ and Δp_i had the unit-slope line been observed.

Step 3 — Determine from the graph the coordinates of the maximum point (peak) on the $t * \Delta p'$ versus time curve, i.e. t_x and $(t * \Delta p')_x$.

Step 4 — Select t_r as discussed in Step 6 of Case 1, and read the corresponding value of Δp_r.

Step 5 — Calculate the permeability from Eq. 2.8.

Step 6 — Calculate the wellbore storage coefficient from Eq. 2.31.

Step 7 — Calculate skin from Eq. 2.34.

Step 8 — Recalculate s from Eqs. 2.27 or 2.28. If the two values of s obtained in Steps 5 and 8 are approximately equal, then k, s and C are correct. If the two values of s are significantly different, which is very possible if there is considerable noise in the derivative curve, then either select a new peak or shift up or down the infinite acting (horizontal) line, and repeat Steps 5, 6 and 7 until the two values of s are approximately equal. Obviously, if needed, the early-time unit slope line can now be drawn.

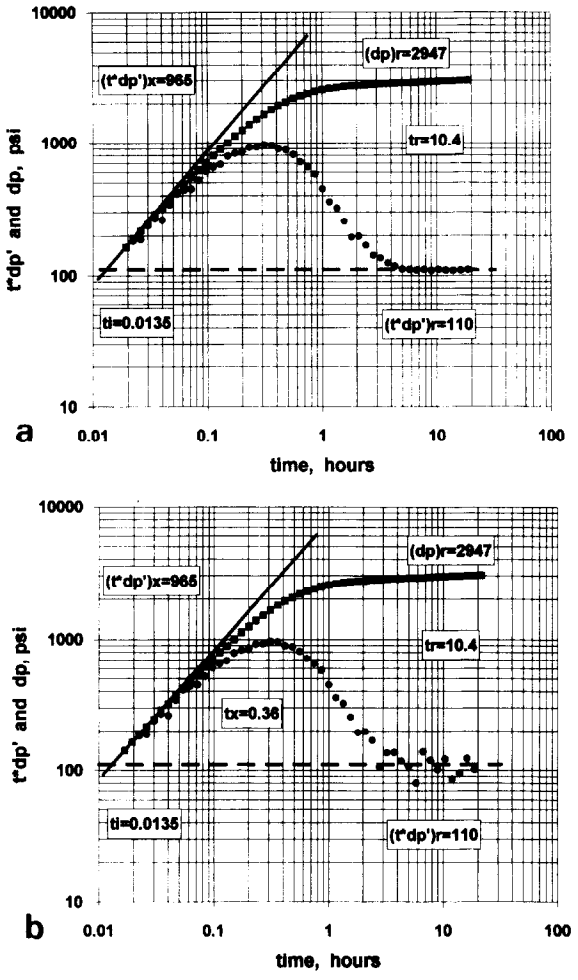

Fig. 2. (a) Pressure and pressure derivative curves for Example 1. The late time portion of the derivative curve is smoothed by the spline technique. (b) Pressure and pressure derivative curves for Example 1. The pressure derivative points were calculated by numerical differentiation.

Example 2

Using the reservoir and well characteristics in Example 1, and the pressure and pressure derivative data in Fig. 3, calculate k, s and C.

Solution

Fig. 3 is actually drawn using the pressure data in Example 1, but without the early-time pressure points. Thus, the coordinates of the maximum point of the wellbore storage hump (Step 3 of this case) are $t_x = 0.36$ h and $(t*\Delta p')_x = 965$ psi. From Step 4, $t_r = 10.4$ h, $\Delta p_r = 2947$ psia, and $(t*\Delta p')_r = 110$ psi. From Step 5 and Eq. 2.8 the permeability is 77.6 md. The wellbore storage coefficient is obtained from Eq. 2.31 (Step 6), which gives $C = 0.0154$ bbl/psi.

From Step 7, the skin factor is approximately 6.2. Eq. 2.30 (Step 8) gives a k value of 77.4 md. Thus, the values of k, s and C are correct.

3.3. Case 3 — The infinite acting line is not observed (short test)

If the pressure test is too short to observe the infinite acting radial flow line, or there is too much scatter in the late-time derivative points, or the boundary effects are felt before the infinite acting flow regime is fully developed, then the following step-by-step procedure is recommended.

Step 1 — Plot Δp and $t*\Delta p'$ versus time on a log–log graph.

Step 2 — Draw the early-time unit slope line as discussed in Step 2 of Case 1.

Step 3 — Read the coordinates of the maximum point (peak) i.e. t_x and $(t*\Delta p')_x$.

Step 4 — Calculate the wellbore storage coefficient from Eq. 2.3, where t and Δp are the coordinates of any convenient point on the unit-slope line.

Step 5 — Calculate the permeability from Eq. 2.22.

Step 6 — Calculate the coordinates of the point of intersection of the unit-slope line and infinite-acting line (had the test been run long enough to observe it) from Eqs. 2.16 and 2.17, i.e. $(t*\Delta p')_i$ and t_i.

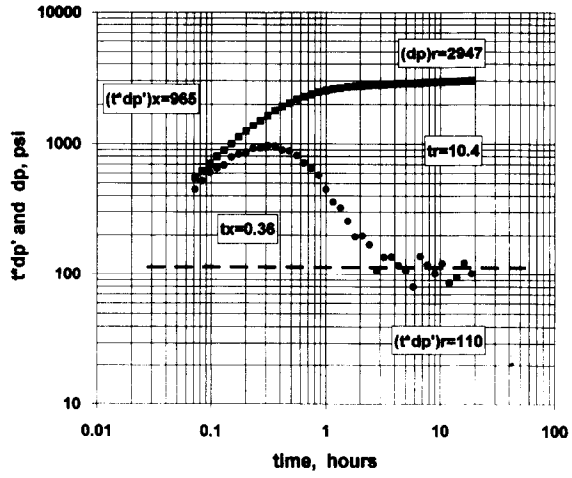

Fig. 3. Pressure and pressure derivative curves for Example 2.

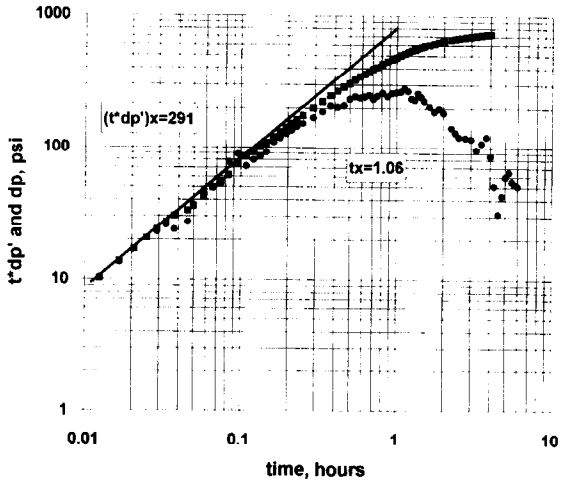

Fig. 4. Pressure and pressure derivative curves for Example 3.

Step 7 — Determine the skin factor from Eq. 2.27 or 2.28.

Step 8 — Recalculate k from Eq. 2.32. If the two values of k obtained in Steps 5 and 8 are approximately equal, then k, s and C are correct. If not, obtain a new peak and/or shift the unit slope line (left or right) and repeat the process until the two values of k obtained from Eqs. 2.21 and 2.32 are approximately identical. If needed, the infinite acting radial line can now be drawn.

Example 3

Using the reservoir, well characteristics and the pressure buildup data in Example 1 of Bourdet et al. (1983), calculate k, s and C.

$q = 174$ STB/D, $\phi = 0.25$,

$\mu = 2.5$ cp, $c_t = 4.2 \times 10^{-6}$ psi^{-1},

$B = 1.06$ RB/STB, $h = 107$ ft,

$r_w = 0.29$ ft

Solution

Fig. 4 is log–log plot of Δp and $t * \Delta p'$ versus test time, without the late-time points (to illustrate the procedure of Case 3). From Step 4 and Eq. 2.3, the wellbore storage coefficient is calculated at $t = 0.1$ h and $\Delta p = 83$ psi. Thus, $C = 9.3 \times 10^{-3}$ bbl/psi.

From Step 5 and Eq. 2.22, the permeability is 10.5 md.

From Step 6, the coordinates of the point of intersection of the unit-slope and infinite acting line are:

$t_i = 0.035$ h, $(t * \Delta p')_i = 28.97$ psi

The skin factor is computed from Eq. 2.27 or 2.28 (Step 7). Using Eq. 2.27, $s = 8.3$.

Eq. 2.28 also gives a skin factor of approximately 8.3. For further verification (Step 8), the permeability is recalculated from Eq. 2.32, where $(t * \Delta p')_r = (t * \Delta p')_i = 28.97$ psi. This equation yields $k = 10.5$ md, which is the same value obtained in Step 5. The values of k, C and s obtained here are approximately equal to the values obtained by type-curve matching and semilog analysis (Bourdet et al., 1983).

3.4. Case 4 — The unit-slope line and the peak are not observed

In some pressure tests, the first pressure reading occurred well after the end of wellbore storage flow regime, such that the peak or maximum point of the pressure derivative is not observed. In this case, if the pressure test is run long enough to observe the infinite acting radial flow (horizontal) line the following procedure is recommended.

Step 1 — Plot Δp and $t * \Delta p'$ versus time on a log–log graph.

Step 2 — Draw the infinite acting radial flow (horizontal) line. The straight line of course has a constant value on the pressure derivative axis $(t * \Delta p')_r$.

Step 3 — Determine from the graph the starting time, t_{SR}, of the infinite acting line of the pressure derivative curve.

Step 4 — Determine Δp_r as discussed in Step 6 of Case 1.

Step 5 — Calculate the permeability from Eq. 2.8.

Step 6 — Calculate the skin factor from Eq. 2.34.

Step 7 — Calculate the dimensionless time at the start of the infinite acting line, t_{DSR}, from Eq. 1.5 where $t = t_{SR}$; then estimate the wellbore storage coefficient from Eq. 2.13.

The starting time t_{SR} is almost impossible to determine, if there is too much noise in the infinite acting portion of the pressure derivative curve. In this case the following procedure is recommended:

(1) Calculate k from the conventional semilog analysis,

(2) Compute $(t * \Delta p')_r$ from Eq. 2.8,

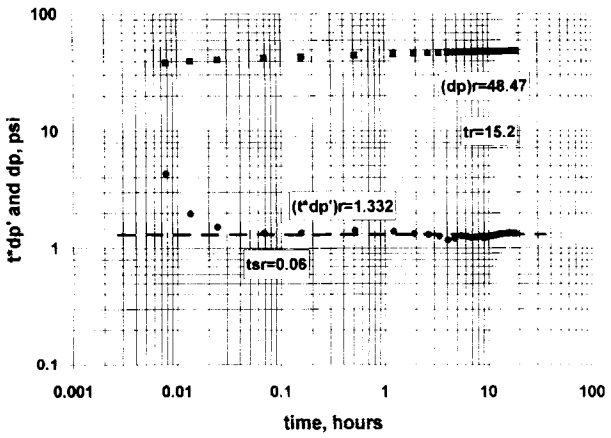

Fig. 5. Pressure and pressure derivative curves for Example 4.

(3) Calculate s from Eq. 2.34, where t_r and Δp_r are determined as discussed above, and

(4) Calculate C from Eq. 2.13 where t_{SR} is obtained from the semilog plot.

Example 4

A pressure buildup test in the Ness formation sand of the Osberg Field, North Sea, is influenced by skin and wellbore storage. The measured shut-in pressure and $t*\Delta p'$ data as a function of time are listed in Table 3 of Clark and Van Golf-Racht (1984). Other reservoir, fluid and well characteristics are listed below:

$q = 3000$ STB/D, $\phi = 0.23$,

$\mu = 0.445$ cp, $c_t = 16.8 \times 10^{-6}$ psi^{-1},

$B = 1.49$ RB/STB, $h = 33$ ft,

$r_w = 0.51$ ft

Solution

Fig. 5 is a log–log plot of Δp and $t*\Delta p'$ versus test time. Using the instructions in Steps 1 through 4 of Case 4, we have: $(t*\Delta p')_r = 1.332$ psi, $\Delta p_r = 48.47$ psi, $t_r = 15.2$ h and $t_{SR} = 0.06$ h.

Using Eq. 2.8 (Step 5), the permeability is 3195 md. Eq. 2.34 (Step 6) gives a skin value of 9.2. The wellbore storage coefficient is computed from Eq. 2.13 (Step 7) and is equal to 6.7×10^{-3} bbl/psi. The values of C and s obtained here are similar to those obtained by Clark and Van Golf-Racht. The values of k are however different (3115 md).

3.5. Case 5 — The unit-slope and infinite-acting lines have not been observed

In some short tests, both the unit slope line and the infinite acting radial flow line are missing. In other tests the first pressure reading was taken after the unit-slope line. For wells with wellbore storage and skin producing from a small bounded reservoir it is possible for boundary effects to be felt before the infinite acting line develops. In these situations, the pressure test can be analyzed as in Case 2 or Case 3, depending on the quality of early and/or late time pressure derivative values. If the wellbore storage coefficient can be calculated from well completion data, then the following procedure is recommended:

Step 1 — Plot Δp and $t*\Delta p'$ versus time on a log–log graph.

Step 2 — Estimate the wellbore storage coefficient from well completion data. For a wellbore with changing liquid level $C = 144 V_u/\rho$, where V_u is the wellbore volume per unit length. When the wellbore is completely filed with a single phase fluid $C = c_w V_w$, where V_w is the total wellbore volume and c_w is the compressibility of the fluid in the wellbore.

Step 3 — Obtain the coordinates of the maximum point (peak) from the derivative curve: t_x and $(t*\Delta p')_x$.

Step 4 — Calculate permeability from Eq. 2.22a.

Step 5 — Calculate $(t*\Delta p')_i$ and t_i from Eqs. 2.16 and 2.17, respectively. If needed, draw the infinite acting line portion of the derivative curve, and the unit slope line.

Step 6 — Calculate the skin factor from Eq. 2.27 and 2.28. If they give different values of s, obtain a new peak and recalculate s until the two equations agree (within 5 percent).

If permeability is known from other sources, then calculate C from Eq. 2.22b and skin as discussed in Steps 5 and 6 (Case 5).

Example 5

Fig. 6 shows pressure and pressure derivative data of a highly damaged well. Calculate the wellbore storage coefficient, permeability and skin. Known reservoir, fluid and well properties are:

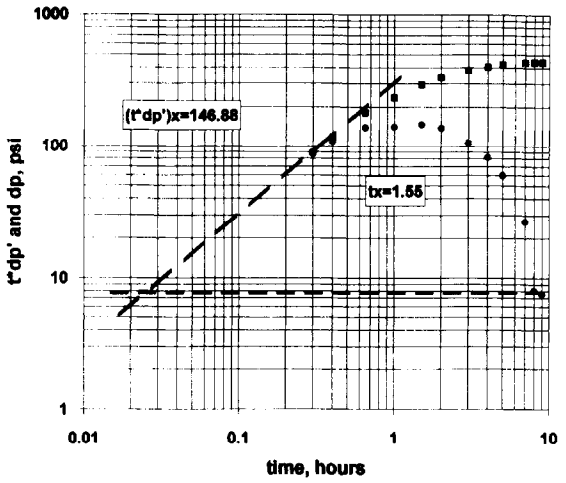

Fig. 6. Pressure and pressure derivative curves for Example 5.

$q = 250$ STB/D, $\phi = 0.18$,
$\mu = 1.2$ cp, $c_t = 2.4 \times 10^{-6}$ psi^{-1},
$B = 1.229$ RB/STB, $h = 16$ ft,
$r_w = 3.2$ in., $\rho = 42.5$ lbm/cuft,
$V_u = 0.0134$ bbl/ft

Solution

From Step 2, the wellbore storage coefficient is $C = 144 \times 0.0134/42.5 = 0.0454$ bbl/psi. The coordinates of the maximum point are $t_x = 1.55$ h and $(t * \Delta p')_x = 146.88$ psi. From Eq. 2.22 (Step 4), the permeability is 206 md. The values of t_i and $(t * \Delta p')_i$ are, respectively, 0.028 h (Eq. 2.17) and 7.88 psi (Eq. 2.16). The skin factor is 19.2 from both Eqs. 2.27 and 2.28.

4. Conclusions

1. A log–log plot of pressure and pressure derivative versus time can be analyzed without using the type-curve matching technique.
2. This new technique is particularly useful when the early-time unit slope line and/or the late-time infinite acting radial flow line have not been observed or are not well defined due to a variety of reasons, such as lack of points, severe noise problem, and interference of outer boundaries.
3. Several unique features of the pressure derivative plot have been identified, including the point of intersection of the unit slope and the infinite acting lines, the maximum point (or peak) or the transition period, and the starting time of the infinite acting line.
4. Equations corresponding to these unique features have been derived and their usefulness has been demonstrated.
5. Unlike type-curve matching, the results of the new technique are verifiable. Any two parameters calculated from two independent equations corresponding to two different features of the pressure derivative curve are verified by a third equation which corresponds to a third feature relating the two parameters.
6. The technique is presented as a step-by-step procedure for five different cases. Each case is illustrated by a numerical example.
7. The spline technique should be used to smooth the pressure derivative curve, especially the portions corresponding to the peak of the wellbore storage hump and the infinite acting radial flow line.
8. The new technique is applicable to the interpretation of pressure drawdown and buildup tests.

5. Nomenclature

b_x	See Eq. 2.21
c_t	Total system compressibility, psi^{-1}
C	Wellbore storage coefficient, RB/psi
C_D	Dimensionless storage constant
h	Formation thickness, feet
$J_0(u)$	Bessel function of the first kind, order zero
$J_1(u)$	Bessel function of the first kind, order one
k	Formation permeability, and
P_D	Dimensionless wellbore pressure drop
P_D'	Dimensionless wellbore pressure derivative
p_i	Initial pressure, psi
p_{wf}	Wellbore flowing pressure, psi
q	Surface rate, STB/day
r_w	Wellbore radius, ft
s	Skin factor
t	Test time, h
t_D	Dimensionless time

t_{DSR} Dimensionless time reflecting time at which storage effects can be assumed to be negligible or start of infinite acting line
$Y_0(u)$ Bessel function of second kind, order zero
$Y_1(u)$ Bessel function of second kind, order one
α Tolerance, fraction
μ Viscosity, cp
ϕ Porosity, fraction of bulk volume

Subscripts

D Dimensionless quantity
i Initial conditions or intersection
w Well
wf Flowing conditions
ws Shut-in condition
x Maximum point or peak
r radial flow
SR Start of radial flow line

Acknowledgements

This paper was originally presented as SPE 25426 at the 1993 SPE Production Operations Symposium held March 21–23 in Oklahoma City, Oklahoma.

References

Agarwal, R.G., Al-Hussainy, R. and Ramey, H.J., Jr., 1970. An investigation of wellbore storage and skin effect in unsteady liquid flow: I. Analytical treatment. Soc. Pet. Eng. J.: 279–290.

Bourdet, D., Whittle, T.M., Douglas, A.A. and Pirard, Y.M., 1983. A new set of type curves simplifies well test analysis. World Oil: 95–106.

Bourdet, D. et al., 1989. Use of pressure derivative in well test interpretation. SPE Form. Eval.: 293.

Clark, G. and Van Golf-Racht, T.D., 1984. Pressure derivative approach to transient test analysis: a high permeability north sea reservoir example. Paper SPE 12959, European Petr. Conf., London, England, Oct. 25–28.

Earlougher, R.C., Jr. and Kersch, K.M., 1974. Analysis of short-time transient test data by type-curve matching. J. Petrol. Tech.: 793–800.

Horne, R.N., 1990. Modern Well Test Analysis. Petroway Inc., Palo Alto, CA.

Lane, H.S. et al., 1991. An algorithm for determining smooth, continuous pressure derivatives from well test-test data. SPE Form. Eval.: 493.

Mishra, S. and Ramey, H.J., 1988. A new derivative type-curve for pressure buildup analysis with boundary effect. J. Petr. Sci. Eng.: 271–275.

Onur, M. and Reynolds, A.C., 1988. A new approach for constructing derivative type curves for well test analysis. SPE Form. Eval.: 197–206.

Ozkan, E., Vo, D.T. and Raghavan, R., 1987. Some applications of pressure derivative analysis procedure. SPE 16811, 62nd Annual Conf. of SPE, Dallas, TX, Sept. 27–30.

Puthigai, S.K and Tiab, D., 1982. Application of P_D' function to vertically fractured wells-field cases. Paper SPE 11028 presented at the SPE 5th Annual Fall Meeting, New Orleans, LA, Sept. 26–29.

Ramey, H.J., Jr., 1970. Short-time well test data interpretation in the presence of skin effects and wellbore storage. J. Petrol. Tech.: 97–104.

Ramey, H.J., Jr. and Agarwal, R.G., 1972. Annulus unloading rates as influenced by wellbore storage and skin effect. Soc. Pet. Eng. J.: 453–462.

Tiab, D., 1975. A new approach (pressure derivative) to detect and locate multiple reservoir boundaries by transient well pressure data. M.S. Thesis, New Mexico Tech.

Tiab, D., 1976. Analysis of multiple-sealing faults systems and bounded reservoirs by type-curve matching (using pressure and pressure derivative). Ph.D. Dissertation, University of Oklahoma.

Tiab, D. and Crichlow, H.B., 1979. Analysis of multiple-sealing fault systems and bounded reservoirs by type curve matching. Soc. Pet. Eng. J.: 378–392.

Tiab, D. and Kumar, A, 1980a. Application of P_D'-function to interference analysis. J. Petrol. Tech.: 1465–1470.

Tiab, D. and Kumar, A., 1980b. Detection of location of two parallel sealing faults around a well. J. Petrol. Tech.: 1701–1708.

Tiab, D., 1989. Direct Type Curve Synthesis. SPE 18992, Proceedings, SPE Rocky Mountain Conf., Denver, Colorado, March.

Tiab, D., 1993. Analysis of pressure and pressure derivatives without type-curve matching — III. Vertically fractured wells in closed systems. SPE 26138, SPE Western Regional Meeting, Anchorage, Alaska, May 26–28.

Vongvuthipornchai, S. and Raghavan, R., 1988. A note on the duration of the transitional period of responses influenced by wellbore storage and skin. SPE Form. Eval.: 207–214.

Wong, D.W., Harrington, A.G. and Cinco-Ley, H., 1986. Application of the pressure-derivative function in the pressure-transient testing of fractured wells. SPE Form. Eval.: 470–480.